Journal of Molecular Structure 1018 (2012) 39–44

Contents lists available at SciVerse ScienceDirect

Journal of Molecular Structure

journal homepage: www.elsevier.com/locate/molstruc

FTIR study of the hydrogen bond symmetry in protonated homodimers of pyridine and collidine in solution

S.M. Melikova [a,*], K.S. Rutkowski [a], A.A. Gurinov [a], G.S. Denisov [a], M. Rospenk [b], I.G. Shenderovich [a,c]

[a] Faculty of Physics, St. Petersburg State University, 1 Ulianovskaia, 198504 Peterhof, St. Petersburg, Russia
[b] Faculty of Chemistry, University of Wrocław, Joliot-Curie 14, 50-383 Wroclaw, Poland
[c] Institute of Organic Chemistry, University of Regensburg, Universitaetsstr. 31, 93040 Regensburg, Germany

ARTICLE INFO

Article history:
Available online 28 December 2011

Keywords:
Hydrogen bonding
FTIR spectra
Homodimers
Pyridine–pyridinium complex
Collidine–collidinium complex

ABSTRACT

FTIR spectra of the protonated homodimers of pyridine and of 2,4,6-trimethylpyridine in solution in dichloromethane have been studied in the temperature interval from 290 to 160 K. It was found that the frequencies of the symmetrical and antisymmetrical CN vibrations are affected by hydrogen bonding strong enough to discriminate between the spectral pattern of hydrogen bonded and protonated pyridines. The experimental results obtained confirm asymmetric structure of both the systems even in low-polar solvent. Optimized structure, energy, vibrational spectrum and potential energy profile for proton transfer coordinate have been studied by DFT/B3LYP method. The calculation predicts that for the studied homodimers the proton transfer coordinate is involved not only in the stretching vibration ν(NH), but also in the rings vibrations ν(CN). As a result, inside a certain interval of the N···H distances the frequency of ν(CN) band should be strongly affected by H/D substitution.

1. Introduction

Proton transfer is the essential step of many chemical reactions. In biological systems this process is often controlled by small changes in the surrounding [1]. As a result, the hydrogen bond responsible for the proton transfer should be strong [2]. Protonated homodimers of pyridines are the simplest model systems to demonstrate this effect. The equality of the proton affinities of the partners is responsible for the strength of the hydrogen bond, while the electronegativity of the sp^2-hybridized nitrogen is insufficient to stabilize the structure with a symmetrical hydrogen bond [3]. The structure and the spectral properties of the protonated homodimers of pyridines were studied in numerous papers [4–11]. Theoretical calculations predict that the aromatic rings of the protonated homodimer of pyridine (Py), [Py-H···Py]$^+$, are oriented perpendicular to each other, and the hydrogen bond is linear with the N···N distance of 2.64 Å [12]. The expected barrier for proton transfer can be as low as 4 kJ/mol [13]. However, in these simulations the effects of both a counterion and the surrounding on the structure of the cation were neglected. These additional interactions can have a remarkable effect [14,15], and in the particular case of charged hydrogen bonded species can result in a contraction of the hydrogen bond [16]. Experimental studies of [Py-H···Py]$^+$ in its complex with a poorly coordinating anion in the crystalline phase indicated that the hydrogen bond was slightly bent. By combining X-ray diffraction analysis with model calculations, the position of the binding proton was defined as r(N–H) = 1.123 Å and r(H···N) = 1.532 Å [17].

NMR studies of the [Py-H···Py]$^+$ system in a polar aprotic solvent has shown that the binding proton is resonated at 21.73 ppm that was above any value reported in the past [18]. Although a part of this downfield shift can be attributed to the ring current effect [19], this value is indicative for a very strong hydrogen bond. Also the value of the primary isotope effect on the H/D chemical shifts was close to the highest ever measured, −0.95 ppm [20,21]. The negative sign of the effect showed that the energy profile for the proton longitudinal vibration had two minima of the same depth [22], while the multiplicity of the ^{1}H resonance indicated that a reversible proton transfer was very fast in the high resolution NMR time scale of milliseconds down to 120 K [17].

Apart the [Py-H···Py]$^+$ system, the protonated homodimer of 2,4,6-trimethylpyridine (sym-Collidine, Col) has been intensively studied by the NMR technique. In contrast to bulky tertbutyl substituents in the ortho positions, the presence of the methyl ones does not prevent the formation of stable hydrogen bonded complexes [23,24]. However, the methyl substituents measurably affect the geometry of hydrogen bridges [25]. For the protonated homodimer of collidine this effect can be demonstrated using the NMR parameters [26]. The binding proton resonated at 19.93 ppm and a primary high-field shift of −0.81 ppm was observed upon deuteration. These values show that the length of the N···N

* Corresponding author.
E-mail address: melikova@molsp.phys.spbu.ru (S.M. Melikova).

0022-2860/$ - see front matter © 2011 Elsevier B.V. All rights reserved.
doi:10.1016/j.molstruc.2011.12.027

distance in $[Col\text{-}H\cdots Col]^+$ is longer as compared to the one in $[Py\text{-}H\cdots Py]^+$. At the same time the rate constant of the reversible proton transfer in the former complex exceeded the value of $10^5\ s^{-1}$ even at relatively low temperature of $T \sim 110$ K [25].

Early IR studies of the protonated homodimer of pyridine [27–29] were not able to provide quantitative information on the structure of the complex in solution and the rate constant of the proton transfer. The N–H stretching is presumably strongly coupled with some other vibrations [27,30] and cannot be used to characterize the features of the hydrogen bond. There are only several reports on the IR spectra of the cation $[Py\text{-}H]^+$ [31–33]. The data, related to the IR spectra of Py and Col, have been shortly discussed in a few works [34,35]. One of the first incomplete results on IR spectra of protonated homodimer of collidine was reported in Ref. [36]. Finally, as to our knowledge, literature data on the IR spectra of the cation $[Col\text{-}H]^+$ are practically absent.

The main goal of this study is to inspect the effect of hydrogen bonding on the IR spectral patterns of Py and Col and to identify characteristic vibrations which can be used to estimate the structural and dynamic parameters of hydrogen bonded complexes involving the pyridines. Specifically, we aim to use for these purposes N–C skeleton vibrations of the aromatic ring. The IR absorption of $[Py\text{-}H\cdots Py]^+$, $[Col\text{-}H\cdots Col]^+$ homodimers and respective monomers have been studied to characterize the effect of hydrogen bonding on the spectral pattern. In the past, IR studies of $[PyH\cdots Py]^+$ have been performed in solution in pyridine at room temperature [27–29]. At these conditions the vibrational bands studied are overlapped by numerous relatively strong bands of Py solvent, making the analysis more difficult. Thus, in the present work, the measurements and spectroscopic analysis have been performed in relatively diluted solutions in CH_2Cl_2 in a wide temperature range from 290 K to 160 K.

Finally, the spectroscopic parameters of the isolated homodimers and cations have been obtained in a series of DFT calculations and used to attribute the experimental data obtained. The effect of proton transfer on the spectroscopic parameters of selected bands attributed to the ring vibrations have been examined by the help of single point calculations of the potential energy along the proton transfer coordinate.

2. Experimental and computational methods

$[Py\text{-}H\cdots Py]^+\ [BF_4]^-$ and $[Col\text{-}H\cdots Col]^+\ [BF_4]^-$ crystals were prepared as follows. Pyridine (120.9 μl, 118.5 mg) and HBF_4 (186.8 μl, 263.4 mg, 50% aq.) were mixed in dichloromethane and stirred for 3 h at 30 °C. Dichloromethane and water were then removed by repeated azeotropic distillation leaving a solid product. Collidine (199.5 μl, 181.5 mg) and HBF_4 (186.8 μl, 263.4 mg, 50% aq.) were mixed in dichloromethane and stirred for 3 h at 30 °C. Dichloromethane and water were then removed by repeated azeotropic distillation leaving a solid product.

FTIR spectra of Py, Col and $[Py\text{-}H\cdots Py]^+$, $[Col\text{-}H]^+$, $[Col\text{-}H\cdots Col]^+$ with $[BF_4]^-$ as the counterion in solution in CH_2Cl_2 were recorded using Nicolet Nexus and partly Bruker IFS-28 Fourier Transform spectrometers in a frequency domain from 400 to 4000 cm^{-1} with resolution of 1 cm^{-1}. Temperature measurements from 290 K to 160 K were performed in a home made low temperature cell with KRS-5 windows and an optical path length of ~50 μ, mounted in a variable temperature Specac cryostat with temperature stabilization better than 0.1 K. The concentration of the solutions was about 0.1 M. We are aware that $[BF_4]^-$ cannot be regarded as totally inert towards conjugated cations [37]. However, the binding protons in the complexes under study are strongly protected from the surrounding by the aromatic rings and bulky $[BF_4]^-$ cannot affect the structure of the corresponding hydrogen bonds remarkably.

As it was mentioned above, the effect of highly polar solvent on charged homodimer has been considered in Ref. [16]. According to the cited work, the decrease of temperature (and thus, an increase of the dielectric permittivity) results in contraction of the hydrogen bond combined with a decrease of hydrogen bridge asymmetry. Since CH_2Cl_2 belongs to the class of inert solvents of a low polarity, the effect of this solvent on the hydrogen bonds studied is of minor importance. We observed only ordinary spectroscopic changes related with bulk intermolecular interactions and temperature lowering (narrowing and weak low frequency shift of majority of the bands registered).

The results obtained for $[Py\text{-}H\cdots Py]^+$ homodimer have been compared with those obtained for a weaker complex formed between $[Py\text{-}H]^+$ and acetonitrile (AN). The latter system was studied only at room temperature in a standard IR cell with a path length of 610 μ.

Optimized geometries and vibrational spectra in harmonic approximation of isolated Py, $[Py\text{-}H]^+$, $[Py\text{-}H\cdots AN]^+$, $[Py\text{-}H\cdots Py]^+$ and Col, $[Col\text{-}H]^+$, $[Col\text{-}H\cdots Col]^+$ were calculated using the GAUSSIAN 03 [38] at the B3LYP/6-31++G(d,p) and B3LYP/6-31G(d,p) levels, respectively. Equilibrium geometries and binding energies of the complexes have been obtained by using the *a priori* BSSE correction method, i.e. CP-corrected gradient techniques [39]. Relaxed potential energy surfaces (PES) scan calculations (with geometry optimization and using CP-corrected gradient techniques at each point) for the proton transfer in $[Py\text{-}H\cdots Py]^+$ were calculated at the B3LYP/6-31++G(d,p) level, while in $[Col\text{-}H\cdots Col]^+$ at the B3LYP/6-31G(d,p) level with the step size 0.02 Å.

3. Results and discussion

The schematic representation of the lowest-energy structure of the protonated homodimers of pyridines including the numbering of atoms is depicted in Fig. 1. The dihedral angle between the pyridine rings is 90°. It should be noted, that dimer $[PyH\cdots Py]^+$ has only one stable structure of C_{2v} symmetry. In the case of $[Col\text{-}H\cdots Col]^+$ one might expect a large number of conformers depending on mutual orientations of CH_3-groups. In the present work only the structure which corresponds to the global minimum on PES has been taken into account. Calculated geometry parameters, the BSSE corrected binding energy E_e^{BSSE} and the ground-state energy adjusted by the zero-point energy ΔZPE E_0 for the most stable structures are collected in Table 1. In the case of $[Py\text{-}H\cdots Py]^+$ the absolute value of E_0 is larger than the absolute value of E_e^{BSSE} because strong decrease of the frequency ν(NH) by complex formation is not compensated by low-frequency intermolecular vibrations.

The results of the relaxed PES scan calculations for the proton transfer are shown in Fig. 2. The proton transfer coordinate is defined as the displacement of the proton with respect to the center of mass of the dimer: $\Delta r(H) = (r_1(N_3H_2) - r_2(N_1H_2))/2$, and was varied from −0.4 Å to +0.4 Å. These simulations have shown that the BSSE corrected barrier for the proton transfer is 6.87 kJ/mol for $[Py\text{-}H\cdots Py]^+$. The barrier is ~2 times higher in the case of $[Col\text{-}H\cdots Col]^+$ (16.75 kJ/mol).

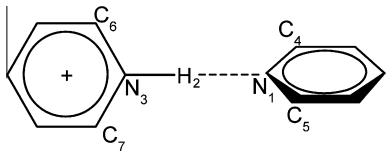

Fig. 1. Schematic representation of the lowest-energy structure of the protonated homodimers of pyridines.

Table 1
Selected calculated geometry parameters (in Å) and the binding energy (in kJ/mol) of $[Py\text{-}H\cdots Py]^+$, $[Py\text{-}H\cdots AN]^+$ and $[Col\text{-}H\cdots Col]^+$.

	B3LYP/6-31++G(d,p)				B3LYP/6-31G(d,p)		
	$[PyH]^+$	Py	$[PyH\cdots Py]^+$	$[PyH\cdots AN]^+$	$[ColH]^+$	Col	$[ColH\cdots Col]^+$
$r_1(N_3H_2)$	1.018		1.111	1.047	1.016		1.083
$r_2(N_1H_2)$			1.574				1.698
$q_1(C_{6,7}N_3)$	1.353		1.3475	1.349	1.362		1.357
$q_2(C_{4,5}N_1)$		1.341	1.3465			1.343	1.351
$R(N_1\cdots N_3)$			2.685	2.806			2.781
E_e^{BSSE}			−118.99	−89.45			−94.05
E_0			−119.29	−86.90			−92.55

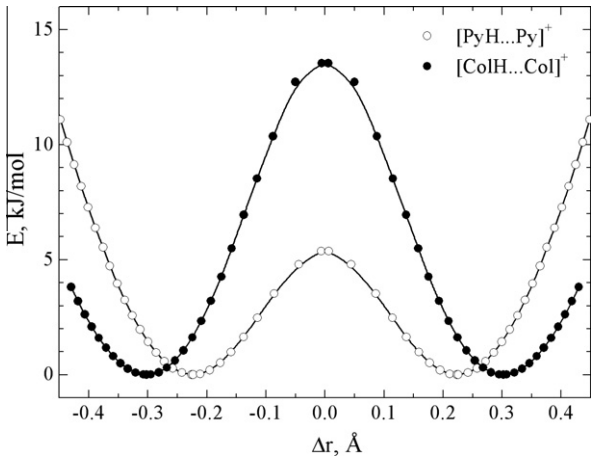

Fig. 2. Calculated potential energy shape for proton transfer for protonated homodimers $[Py\text{-}H\cdots Py]^+$ and $[Col\text{-}H\cdots Col]^+$.

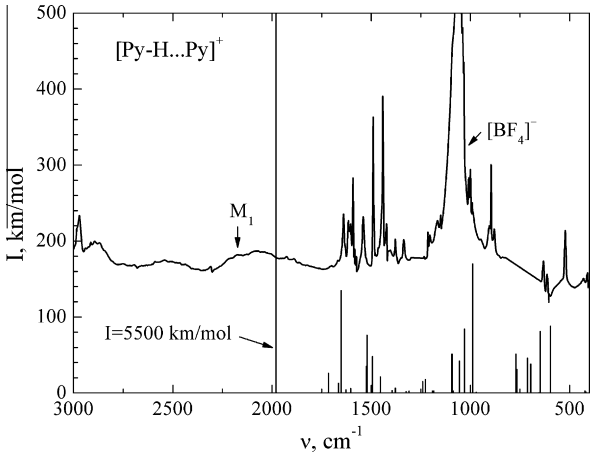

Fig. 3. Selected region of a FTIR absorption spectrum and the calculated vibrational transitions of $[Py\text{-}H\cdots Py]^+$ (shown by sticks). Solution in CH_2Cl_2, T = 160 K, L = 50 μ. The marker at 2160 cm^{-1} corresponds to the first spectral moment of the ν(NH) stretching vibration. The band of BF_4^- counterion and the intensity of the calculated ν(NH) band are marked by arrows.

Figs. 3 and 4 present the experimental IR spectra of $[Py\text{-}H\cdots Py]^+$ and $[Col\text{-}H\cdots Col]^+$. Also the spectra calculated in harmonic approximation are shown by sticks. The experimental and calculated frequencies and calculated intensities of selected vibrations related with hydrogen bridge motion are collected in Tables 2 and 3. The calculated frequencies are presented without correction on scaling factor k_{sc} (usually k_{sc} varies from 0.9 to 1 in spectral range 3000–400 cm^{-1}). This feature, together with the fact that the calculated

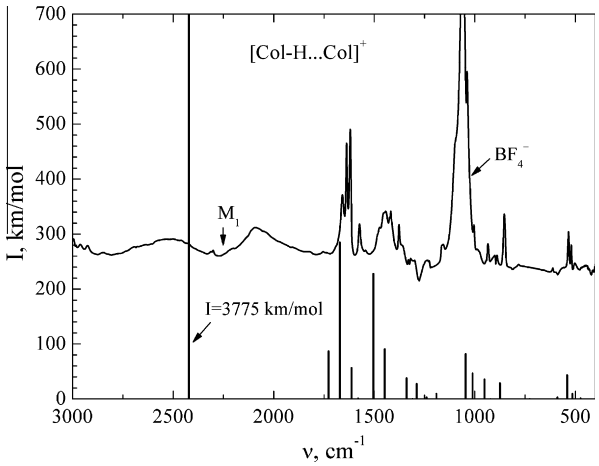

Fig. 4. Selected region of a FTIR absorption spectrum and the calculated vibrational transitions of $[Col\text{-}H\cdots Col]^+$ (shown by sticks). Solution in CH_2Cl_2, T = 180 K, L = 60 μ. The marker at 2250 cm^{-1} corresponds to the first spectral moment of the ν(NH) stretching vibration. The band of BF_4^- counterion and the intensity of the calculated ν(NH) band are marked by arrows.

intensities are roughly coincide with the experimental ones, simplifies the attribution of the experimental bands.

For both protonated homodimers the large amplitude stretching vibration ν(NH) (ν_{13} in Tables 2 and 3), which predominantly relates to the motion of the bridging proton, is registered as a broad doublet-like band. The first spectral moments (M_1) of this noticeably broadened band amount 2160 cm^{-1} and 2250 cm^{-1} for $[Py\text{-}H\cdots Py]^+$ and $[Col\text{-}H\cdots Col]^+$, respectively, that is the hydrogen bond in the former cation is stronger and shorter as compared to the latter one. In most cases the trend of the observed effects is the same for both $[Py\text{-}H\cdots Py]^+$ and $[Col\text{-}H\cdots Col]^+$. For this reason we discuss below mainly $[Py\text{-}H\cdots Py]^+$ and compare it to $[Col\text{-}H\cdots Col]^+$ only to highlight essential differences.

The description of the normal vibrations in Tables 2 and 3 was done in accordance with the calculated L-matrix. One can see from the tables that most of the vibrations are not characteristic. Totally symmetric (A_1) vibrations ν_6, ν_{10}, ν_{11}, ν_{13} have contributions from symmetrical stretching internal modes of the rings ($q^s(CN)_{PyH+}$, $q^s(CC)_{PyH+}$, $q^s(CN)_{Py}$, $q^s(CC)_{Py}$) and longitudinal proton motion mode r(NH). In contrast, vibrations of symmetry B_1 (ν_3, ν_4, ν_8, ν_{12}) and B_2 (ν_2, ν_5, ν_9) involve antisymmetrical stretching motions of the rings ($q^{as}(CN)_{PyH+}$ and $q^{as}(CN)_{Py}$) and bending (in plane and out of plane) displacements of the proton δ(NH) and γ(NH).

One can suggest that the frequencies of vibrations ν_{10} and ν_{11} might noticeably depend on the degree of asymmetry of the hydrogen bridge due to the coupling of the longitudinal proton displacement mode and the internal stretching modes of the rings.

In order to examine this suggestion, we calculate the dependences of frequencies ν(CN) (ν_{10}, ν_{11}) and ν(NH) (ν_{13}) vibrations on the N···N distance that is reciprocally proportional to the

Table 2
Experimental and calculated frequencies and calculated intensities of selected normal vibrations of $[Py\text{-}H\cdots Py]^+$. Calculation at the B3LYP/6-31++G(d,p) level.

Vibr.	Description[a]	W.n.[b]	Sym	ν (cm^{-1})		I (km/mol)
				Calc	Exp 160 K	Calc
ν_1	ν_θ (N···N)		A_1	139	138[c]	76
ν_2	γ(NH) + $q^{as}(CN)_{Py}$ + $q^{as}(CC)_{Py}$	14(2)	B_2	1310		2.4
ν_3	δ(NH) + $q^{as}(CN)_{PyH+}$ + $q^{as}(CC)_{PyH+}$	14(1)	B_1	1325		1.9
ν_4	δ(NH) + $q^{as}(CC)_{PyH+}$ + $q^{as}(CN)_{PyH+}$	19b(1)	B_1	1454	1422	21
ν_5	γ(NH) + $q^{as}(CC)_{Py}$ + $q^{as}(CN)_{Py}$	19b(2)	B_2	1494	1439	48
ν_6	$q^{s}(CN)_{Py}$ + $q^{s}(CN)_{PyH+}$ + r(NH)	19a(2)	A_1	1521	1490	76
ν_7	$q^{s}(CN)_{PyH+}$ + $q^{s}(CN)_{Py}$ + $q^{s}(CC)_{PyH+}$	19a(1)	A_1	1524		35
ν_8	δ(NH) + $q^{as}(CN)_{PyH+}$ + $q^{as}(CC)_{PyH+}$	8b(1)	B_1	1604	1540	5.8
ν_9	$q^{as}(CN)_{Py}$ + $q^{as}(CC)_{Py}$ + γ (NH)	8b(2)	B_2	1627	1592	4.1
ν_{10}	$q^{s}(CN)_{Py}$ + $q^{s}(CC)_{Py}$ + r(NH)	8a(2)	A_1	1651	1603	135
ν_{11}	$q^{s}(CN)_{PyH+}$ + $q^{s}(CC)_{PyH+}$ + r(NH)	8a(1)	A_1	1665	1615	13
ν_{12}	δ(NH) + $q^{as}(CN)_{PyH+}$		B_1	1715	1639	26
ν_{13}	r(NH) + $q^{s}(CN)_{PyH+}$ + $q^{s}(CC)_{PyH+}$		A_1	1980	2160[d]	5500

[a] r, q^s – Symmetrical stretching, q^{as} – antisymmetrical stretching, δ – bending in plane, γ – bending out of plane of pyridinium ring.
[b] Vibrational assignments for the aromatic rings have been made on the basis of Wilson notation [31], (1) and (2) refer to $[Py\text{-}H]^+$ and Py respectively.
[c] Ref. [23].
[d] The first spectral moment of the band (M_1).

Table 3
Experimental and calculated frequencies and calculated intensities of selected normal vibrations of $[Col\text{-}H\cdots Col]^+$. Calculation at the B3LYP/6-31G(d,p) level.

Vibr.	Description	ν (cm^{-1})		I (km/mol)
		Calc	Exp 160 K	Calc
ν_1	ν_θ (N···N)	99		20
ν_2	γ(NH) + $q^{as}(CN)_{Col}$ + $q^{as}(CC)_{Col}$	1310		0.7
ν_3	δ (NH) + $q^{as}(CN)_{ColH+}$ + $q^{as}(CC)_{ColH+}$	1328		16
ν_4	δ(NH) + $q^{as}(CC)_{ColH+}$ + $q^{as}(CN)_{ColH+}$	1445		19
ν_5	$q^{as}(CC)_{Col}$ + γ (NH)	1512		80
ν_6	$q^{s}(CN)_{Col}$ + r(NH)	1519		0.4
ν_7	$q^{s}(CN)_{ColH+}$ + $q^{s}(CC)_{ColH+}$	1525		34
ν_8	δ(NH) + $q^{as}(CN)_{ColH+}$ + $q^{as}(CC)_{ColH+}$	1580		1.4
ν_9	$q^{as}(CN)_{Col+}\gamma$(NH)	1613	1573	57
ν_{10}	$q^{s}(CN)_{Col}$ + $q^{s}(CC)_{Col}$ + r(NH)	1667	1618	180
ν_{11}	$q^{s}(CN)_{ColH+}$ + $q^{s}(CC)_{ColH+}$ + r(NH)	1677	1638	104
ν_{12}	δ(NH) + $q^{as}(CN)_{ColH+}$	1727	1659	87
ν_{13}	r(NH) + $q^{s}(CN)_{ColH+}$	2421	2250[a]	3775

[a] The first spectral moment of the band (M_1).

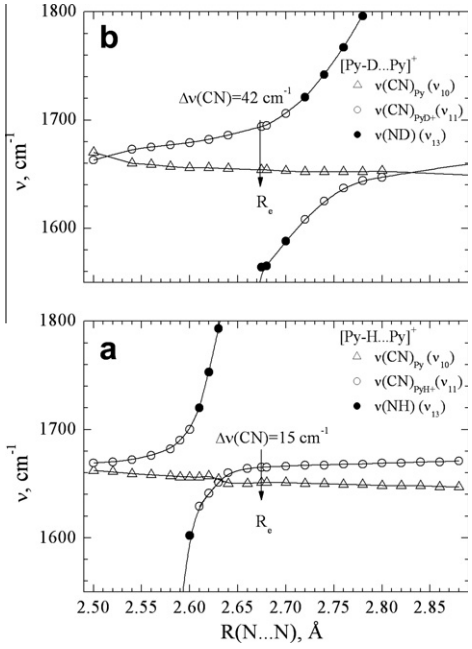

Fig. 5. Calculated dependence of the frequencies $\nu(CN)_{Py}$ (ν_{10}), $\nu(CN)_{PyH+}$ (ν_{11}) and ν(NH/D) (ν_{13}) on the hydrogen bond length R(N···N) for two isotopically substitutions: $[Py\text{-}H\cdots Py]^+$ (a) and $[Py\text{-}D\cdots Py]^+$ (b). R_e = 2.675 Å is the equilibrium length (shown by arrow).

hydrogen bond strength (Fig. 5). At the saddle point of PES, R(N···N) = 2.5 Å, frequencies of two symmetrical ν(CN) vibrations coincide (1662 cm^{-1}). However, only one of them is IR active. The elongation of the N···N distance results in the asymmetrization of the hydrogen bond. This leads to a splitting between the ν_{10} and ν_{11} bands. Upon this elongation the frequency ν_{10} decreases slowly and monotonically. In contrast, the frequency ν_{11} first increases, Fig. 5a. At R(N···N) = 2.61 Å the frequency of ν_{11} coincides with the frequency of ν_{13}. The latter frequency is rapidly increasing with the lengthening of the N···N distance, i.e. with the weakening of the hydrogen bond strength. As a result, at this geometry one obtains the "resonance repulsion" between ν_{11} and ν_{13} vibrations that leads to a dramatic decrease of the ν_{11} frequency below the frequency of the ν_{10} vibration. At the further stretching of the N···N distance the frequency of ν_{11} increases fast above the frequency of ν_{10} and then stabilizes about 15 cm^{-1} above the latter. It is worth to notice that the difference between the frequencies of ν_{10} and ν_{11} at the optimized geometry, R(N···N) = 2.675 Å, is very close to the one observed in experiment, 12 cm^{-1}. This complex behavior of the frequency of ν_{11} as a function of the N···N distance demonstrates that the splitting between the ν_{10} and ν_{11} bands depends on the difference $|\nu_{11} - \nu_{13}|$. The amplitude of this splitting can be most effectively used as a measure of hydrogen bond geometry when the frequency of ν_{13} is approaching the frequency of ν_{11}. In the case of pyridine this situation corresponds to very short and strong hydrogen bonds. However, one can shift the "resonance repulsion" region towards weaker hydrogen bonds by a reduction of the frequency of ν_{13}. This reduction can be easily achieved using the H/D isotope substitution. Indeed, our model calculations predict that the difference between the frequencies of ν_{10} and ν_{11} in $[Py\text{-}D\cdots Py]^+$ at the optimized geometry should be about 40 cm^{-1} (Fig. 5b). We are not aware about other examples of such enormous isotope effect on the skeleton vibrations of hydrogen-bonded molecules. Thus, analyzing the IR spectrum in the range of the stretching vibrations ν(CN), it is quite realistic to obtain the valuable information about the asymmetry degree of the hydrogen bridge.

The effect of complex formation on the frequencies of these vibrations can be demonstrated using the data collected in Tables 4 and 5 and spectra depicted in Figs. 6 and 7. The protonation of collidine (Table 5) results in considerable blue shift $\Delta\nu$ of both

Table 4
Calculated and experimental frequencies (in cm^{-1}) of ν(CN) stretching vibrations in pyridine and its hydrogen-bonded complexes. Calculation at the B3LYP/6-31++G(d,p) level.

System		$[Py\text{-}H\cdots Py]^+$		$[Py\text{-}H]^+$	Py		$[Py\text{-}H...AN]^+$	
Vibr.	Sym	Calc	Exp 160 K	Calc	Calc	Exp 160 K	Calc	Exp 290 K
ν_{11}	A_1	1665	1615	1671			1675	1612
ν_{10}	A_1	1651	1603		1632	1601		
ν_{12}	B_1	1715	1639	1653			1694	1638
ν_8	B_1	1604	1540				1597	1538
ν_9	B_2	1627	1592		1628	1584		

Table 5
Calculated and experimental frequencies of ν(CN) stretching vibrations in collidine and its hydrogen-bonded complexes. Calculation at the B3LYP/6-31G(d,p) level.

Vibr.	$[Col\text{-}H\cdots Col]^+$		$[Col\text{-}H]^+$		Col	
	Calc	Exp 160 K	Calc	Exp 160 K	Calc	Exp 160 K
ν_{11}	1677	1638	1667	1645		
ν_{10}	1667	1618			1660	1612
ν_{12}	1727	1659	1680	1639		
ν_9	1613	1573			1621	1570

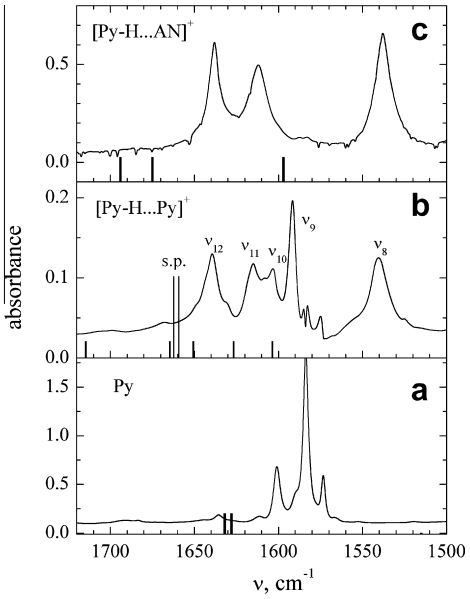

Fig. 6. FTIR spectrum in the region of ν(CN) vibrations of Py (a), $[Py\text{-}H\cdots Py]^+$ (b), and $[Py\text{-}H\cdots AN]^+$ (c). The theoretically predicted frequencies of stable structure of homodimer and saddle point (s.p.) structure (R(N···N) = 2.5 Å) are shown by short and long sticks correspondingly.

the symmetrical and asymmetrical ν(CN) vibrations. For example $\Delta\nu$ reaches a value of +33 cm^{-1} in the case of ν_{11} band of $[Col\text{-}H]^+$ as compared with ν_{10} band of Col. The shift $\Delta\nu$ decreases slightly up to +26 cm^{-1} due to $[Col\text{-}H\cdots Col]^+$ complex formation. This effect correlates with an elongation of N–H bond of $[Col\text{-}H]^+$: Δr = +0.066 Å (see Table 1). The shift $\Delta\nu$ = + 6 cm^{-1} is observed for ν_{10} band of Col in $[Col\text{-}H\cdots Col]^+$ complex. The last might be considered as the model situation which mimics the proton transfer from the left part to the right part of the homodimer. It is reasonable to expect the analogous protonation effect on the respective bands of Py, i.e. noticeable blue shift effect on ν(CN) vibrations of Py due to protonation, and further, weakening the blue shift when going to stronger H–bonded complexes. It is reasonable to suppose that the IR spectroscopic measurements of the frequency of the respective band might be proposed as a convenient tool for detection of the proton displacement (up to the proton transfer) in the hydrogen bridge.

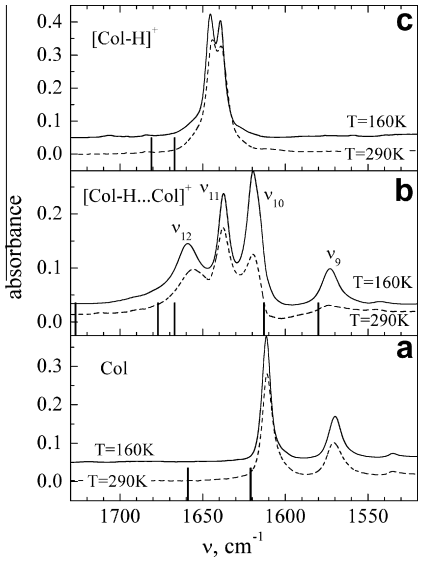

Fig. 7. FTIR spectrum in the region of ν(CN) vibrations of Col (a), $[Col\text{-}H\cdots Col]^+$ (b) and $[Col\text{-}H]^+$ (c). The theoretically predicted frequencies of stable structure of homodimer are shown by sticks.

In the past the correlation of analogous type was established between the N···H distance and the ^{15}N NMR chemical shift of pyridines [40]. The latter correlation reveals to be very useful in material science because the geometry of hydrogen bond can be used as a sensor sensitive to the local structural and chemical properties of amorphous systems [41–45].

The comparison of the spectra of $[Py\text{-}H\cdots Py]^+$ and $[Py\text{-}H\cdots AN]^+$ species (Table 4 and Fig. 6c) is helpful in the assignment of selected bands. Indeed, ν(CN) of the CH_3CN appears in the high frequency range (DFT calculation gives 2376 cm^{-1}), therefore only the vibrations of $[PyH]^+$ fragment contribute in the considered frequency range. The measured splitting between the symmetric vibrations ν_{10} and ν_{11} amounts 12 cm^{-1} at T = 160 K. This value is quite close to the calculated value of 14 cm^{-1}. This is an additional argument which confirms the formation of asymmetric structure of homodimer even in a weakly polar solvent. This is in agreement with the results of model quantum mechanical calculations reported in the past [13], and supplements the results obtained recently for these complexes in the solid state [17].

Finally, the obtained experimental data allowed us to estimate the upper limit of the proton transfer rate in the protonated homodimers of pyridine and collidine. Up to 290 K the IR spectra of both complexes exhibit the sets of bands that are characteristic for a protonated cation and a hydrogen bonded base. Thus, we conclude that the proton transfer rates between the molecules in the protonated homodimers are slow in the IR time-scale. The differences in the skeleton vibrations of the two partner of the same protonated homodimer are of the order of 10 cm^{-1}, that is at least 3×10^{11} Hz. Thus, in aprotic solvents the proton transfer rates in the protonated homodimers of pyridines are slower than 10^{11} s^{-1} up to 290 K. This

conclusion is obvious for [Col-H···Col]$^+$ because the spectral pattern is the same at 290 and 160 K, Fig. 7.

4. Conclusions

In this study, we have examine the effect of hydrogen bonding on the IR spectral patterns of the protonated homodimers of pyridines aiming to identify vibrations that measurably and monotonically depend on the length of the N···H distance. Specifically, the protonated homodimers of pyridine and of 2,4,6-trimethylpyridine in solution in dichloromethane have been studied in the temperature interval from 290 to 160 K. The obtained experimental results demonstrate that the frequencies of the symmetrical and antisymmetrical CN vibrations are affected by hydrogen bonding strong enough to discriminate between the spectral pattern of hydrogen bonded and protonated pyridines. This feature has been used to prove that the [N–H···N]$^+$ hydrogen bonds are asymmetric in both studied homodimers and that the proton transfer rates are slower than 10^{11} s^{-1} up to 290 K.

Although, the amplitude of the effect observed for the studied heterocycles was too small to expect that it is feasible to establish a correlation between the length of the N···H distance and the shift of CN vibrations, strong coupling of these vibrations to CC and NH vibrations makes this shift dependent on the type of the substituents of the aromatic ring. Thus, proper selection of the substituents can amplify the effect.

DFT calculations of relaxed PES as function of the proton transfer reaction coordinate suggest markedly lower barrier for the PT in the case of [Py-H···Py]$^+$ system. Besides that DFT calculations indicate that inside a certain interval of the frequencies of the NH vibration, this vibration strongly affects the frequency of the stretching ν(CN) vibrations of the ring. The frequency of the former vibrations varies in a wide range as a function of the N···H distance. Thus, in a certain interval of N···H distances there should be an enormous H/D isotope effect on the frequency of the ν(CN) bands.

Acknowledgements

The authors acknowledge support from RFBR (Grant No. 11-03-00346a). M.R. thanks NCN (NN 204 150 338) for financial support.

References

[1] J.T. Hynes, J. Klinman, H.H. Limbach, R.L. Schowen (Eds.), Hydrogen—Transfer Reactions, vol. 1–4, Wiley-VCH, Weinheim, 2007.
[2] S.B. Lesnichin, I.G. Shenderovich, T. Muljati, H.-H. Limbach, D. Silverman, J. Am. Chem. Soc. 133 (2011) 11331–11338.
[3] B. Chan, J.E. Del Bene, L. Radom, Mol. Phys. 107 (2009) 1095–1105.
[4] J.L. Wood, J. Mol. Struct. 17 (1973) 307–328.
[5] E. Grech, Z. Malarski, L. Sobczyk, Spectr. Lett. 9 (1976) 749–754.
[6] N.S. Golubev, G.S. Denisov, J. Mol. Struct. 75 (1981) 311–326.
[7] Z. Malarski, L. Sobczyk, E. Grech, J. Mol. Struct. 177 (1988) 339–349.
[8] V.M. Schreiber, M. Rospenk, L. Sobczyk, Chem. Phys. Lett. 304 (1999) 73–78.
[9] W. Tatara, M.J. Wojcik, J. Lindgren, M. Probst, J. Phys. Chem. A 107 (2003) 7827–7831.
[10] L. Sobczyk, J. Mol. Struct. 972 (2010) 59–63.
[11] I. Majerz, I. Olovsson, J. Mol. Struct. 976 (2010) 11–18.
[12] J.E. Del Bene, J. Elguero, J. Phys. Chem. A 110 (2006) 7496–7502.
[13] I.G. Shenderovich, Russ. J. Gen. Chem. 77 (2007) 620–624.
[14] S. Kong, I.G. Shenderovich, M.V. Vener, J. Phys. Chem. A 114 (2010) 2393–2399.
[15] M.V. Vener, S. Kong, A.A. Levina, I.G. Shenderovich, Acta Chim. Slov. 58 (2011) 402–410.
[16] N.S. Golubev, I.G. Shenderovich, P.M. Tolstoy, D.N. Shchepkin, J. Mol. Struct. 697 (2004) 9–15.
[17] S. Kong, A.O. Borissova, S.B. Lesnichin, M. Hartl, L.L. Daemen, J. Eckert, M.Yu Antipin, I.G. Shenderovich, J. Phys. Chem. A 115 (2011) 8041–8048.
[18] H.-H. Limbach, P.M. Tolstoy, N. Perez-Hernandez, J. Guo, I.G. Shenderovich, G.S. Denisov, Israel J. Chem. 49 (2009) 199–216.
[19] I.G. Shenderovich, Russ. J. Gen. Chem. 76 (2006) 501–506.
[20] A. Filarowski, J. Phys. Org. Chem. 18 (2005) 686–698.
[21] M.V. Vener, Chem. Phys. 166 (1992) 311–316.
[22] N.S. Golubev, S.M. Melikova, D.N. Shchepkin, I.G. Shenderovich, P.M. Tolstoy, G.S. Denisov, Z. Phys. Chem. 217 (2003) 1549–1563.
[23] D.V. Andreeva, B. Ip, A.A. Gurinov, P.M. Tolstoy, I.G. Shenderovich, H.-H. Limbach, J. Phys. Chem. A 110 (2006) 10872–10879.
[24] I.G. Shenderovich, P.M. Tolstoy, N.S. Golubev, S.N. Smirnov, G.S. Denisov, H.-H. Limbach, J. Am. Chem. Soc. 125 (2003) 11710–11720.
[25] S. Sharif, I.G. Shenderovich, L. González, G.S. Denisov, D.N. Silverman, H.-H. Limbach, J. Phys. Chem. A 111 (2007) 6084–6093.
[26] P. Schah-Mohammedi, I.G. Shenderovich, C. Detering, H.-H. Limbach, P.M. Tolstoy, S.N. Smirnov, G.S. Denisov, N.S. Golubev, J. Am. Chem. Soc. 122 (2000) 12878–12879.
[27] R. Clements, J.L. Wood, J. Mol. Struct. 17 (1973) 265–282.
[28] S.E. Odinokov, A.A. Mashkovsky, V.P. Glazunov, Spectr. Acta 32A (1976) 355–1363.
[29] S.F. Tayyari, S.J. Mahdizadeh, S. Holakoei, Y.A. Wang, J. Mol. Struct. 971 (2010) 39–46.
[30] B. Brzezinski, G. Zundel, J. Chem. Soc., Faraday Trans. II 72 (1976) 2127–2137.
[31] D. Cook, Can. J. Chem. 39 (1961) 2009–2024.
[32] V.P. Glazunov, S.E. Odinokov, Spectr. Acta 38A (1982) 399–408.
[33] V.P. Glazunov, S.E. Odinokov, Spectr. Acta 38A (1982) 409–415.
[34] J.F. Arenas, I. Lopez Tocon, J.C. Otero, J.I. Marcos, J. Mol. Struct. 476 (1999) 139–150.
[35] J.Z. Frejszar-Olszewska, A.S. Muszynski, J.P. Hawranek, J. Mol. Struct. 404 (1997) 247–256.
[36] R. Clements, J.L. Wood, J. Mol. Struct. 17 (1973) 283–290.
[37] S.B. Lesnichin, P.M. Tolstoy, H.-H. Limbach, I.G. Shenderovich, Phys. Chem. Chem. Phys. 12 (2010) 10373–10379.
[38] M.J. Frisch, G.W. Trucks, H.B. Schlegel, G.E. Scuseria, M.A. Robb, J.R. Cheeseman, J.A. Montgomery, Jr., T. Vreven, K.N. Kudin, J.C. Burant, J.M. Millam, S.S. Iyengar, J. Tomasi, V. Barone, B. Mennucci, M. Cossi, G. Scalmani, N. Rega, G.A. Peterson, H. Nakatsuji, M. Hada, M. Ehara, K. Toyota, R. Fukuda, J. Hasegawa, M. Ishida, T. Nakajima, Y. Honda, O. Kitao, H. Nakai, M. Klene, X. Li, J.E. Knox, H.P. Hratchian, J.B. Cross, C. Adamo, J. Jaramillo, R. Gomperts, R.E, Stratmann, O. Yazyev, A.J. Austin, R. Cammi, C. Pomelli, J.W. Ochterski, P.V. Ayala, K, Morokuma, G.A. Voth, P. Salvador, J.J. Dannenberg, V.G. Zakrzewski, S. Dapprich, A.D. Daniels, M.C. Strain, O. Farkas, D.K. Malick, A.D. Rabuck, K Raghavachari, J.B. Foresman, J.V. Ortiz, Q. Cui, A.G. Baboul, S. Clifford, J. Cioslowski, B.B. Stefanov, G. Liu, A. Liashenko, P. Piskorz, I. Komaromi, R.L. Martin, D.J. Fox, T. Keith, M.A. Al-Laham, C.Y. Peng, A. Nanayakkara, M. Challacombe, P.M.W. Gill, B. Johnson, W. Chen, M.W. Wong, C. Gonzalez, J.A. Pople, Gaussian 03, Revision C.02; Gaussian, Inc., Wallingford, CT, 2004.
[39] S. Simon, M. Duran, J.J. Dannenberg, J. Chem. Phys. 105 (1996) 11024.
[40] P. Lorente, I.G. Shenderovich, N.S. Golubev, G.S. Denisov, G. Buntkowsky, H.-H. Limbach, Magn. Reson. Chem. 39 (2001) S18–S29.
[41] S.B. Lesnichin, N. Kamdem, D. Mauder, G.S. Denisov, I.G. Shenderovich, Russ. J. Gen. Chem. 80 (2010) 2027–2031.
[42] E. Vaganova, E. Wachtel, G. Leitus, D. Danovich, S. Lesnichin, I.G. Shenderovich, H.-H. Limbach, S. Yitzchaik, J. Phys. Chem. B 114 (2010) 10728–10733.
[43] B.C.K. Ip, D.V. Andreeva, G. Buntkowsky, D. Akcakayiran, G.H. Findenegg, I.G. Shenderovich, Micropor. Mesopor. Mater. 134 (2010) 22–28.
[44] D. Mauder, D. Akcakayiran, S.B. Lesnichin, G.H. Findenegg, I.G. Shenderovich, J. Phys. Chem. C 113 (2009) 19185–19192.
[45] I.G. Shenderovich, D. Mauder, D. Akcakayiran, G. Buntkowsky, H.-H. Limbach, G.H. Findenegg, J. Phys. Chem. B 111 (2007) 12088–12096.